The Determination of the Atmospheric Optical Thickness Over Western Europe Using SeaWiFS Imagery

Alexander A. Kokhanovsky, Wolfgang von Hoyningen-Huene, Heinrich Bovensmann, and John P. Burrows

Abstract—The first results obtained from the aerosol-cloud retrieval algorithm (developed at the University of Bremen) are presented. The algorithm enables the observation of the regional characteristics of aerosol and cloud optical thickness both over land and ocean surfaces. The aerosol and cloud optical thickness over Western Europe is derived from the high-resolution SeaWiFS data for October 11, 2001 (11:30 UTC). The most probable value of the aerosol optical thickness was found to be equal approximately 0.25. The frequency distributions of the aerosol and cloud optical thickness are skewed and have long tails for larger optical thickness. It was found that retrieved values of the aerosol optical thickness at wavelengths 0.412 and 0.440 μm are close to those measured by five ground-based instruments placed at different locations. The problems related to the retrieval of the atmospheric optical thickness from space are discussed.

Index Terms—Aerosols, atmospheric optics, clouds, radiative transfer, remote sensing.

I. INTRODUCTION

CLOUDS AND aerosols are important constituents of the atmosphere and in particular of the troposphere. In addition to their unique role in the hydrological cycle of the earth–atmosphere system, they act as both sources and sinks for atmospheric gases in both the stratosphere and troposphere as well as being of significance in determining the radiative balance within the atmosphere. In particular, cloud processes supply and deplete water vapor. Our knowledge about the global behavior of clouds and aerosols is poor and not sufficient to assess the impact of anthropogenic activity on atmospheric chemistry and climate change (e.g., see the Intergovernmental Panel on Climate Change (IPCC) [24]).

The remote sensing of aerosol and cloud fields from the instrumentation aboard space-based platforms provides a unique opportunity to improve our understanding of the global behavior of clouds and aerosols [6]. In particular, the optical thickness τ of terrestrial atmosphere as a function of the wavelength results from these measurements. In the visible spectral region, where the energy of the incident solar flux has a maximum, this parameter is dominant in determining the radiative energy budget of our planet [57].

The atmospheric optical thickness, excluding those spectral regions where atmospheric gases exhibit strong absorption, depends mostly on the column concentration of suspended particles within the atmosphere: the latter comprising, e.g., dust and water-soluble aerosols, cloud droplets and crystals. As τ also depends on the size, shape and chemical composition of particles, the slope of the aerosol optical thickness as a function of the wavelength is an important characteristic, which yields the aerosol type.

Several studies have been devoted to the derivation of the aerosol and cloud optical thickness from measurements of the top-of-atmosphere reflectance, performed by different radiometers and spectrometers on board a variety of satellite platforms [10], [13], [14], [22], [25]–[27], [31], [32], [41], [42], [49]. Aerosol and cloud optical thickness retrievals have mostly been performed by the different groups using different retrieval codes, designed for the retrieval of either cloud or aerosol parameters. However, clouds and aerosols exist in the terrestrial atmosphere simultaneously and also are mutually interdependent [6], [18], [44]. For instance, Breon *et al.* [6] speculate that there is probably an anthropogenic impact on the cloud microphysical and, therefore, radiative properties. This is, in particular, due to the influence of anthropogenic aerosols on cloud droplets spectra and concentrations. The increased droplet number concentration leads to smaller droplet sizes that make precipitation formation more difficult producing larger water contents [1], [17]. Clouds are not passive species in this interaction process. They also influence the aerosol microphysical properties [45].

In summary, it is, therefore, of importance to have combined measurements and retrieval algorithms, which are capable of the simultaneous derivation of both cloud and aerosol optical thickness (and other aerosol and cloud properties) both over ocean and land. Note that current aerosol operational algorithms are mostly restricted to the aerosol optical thickness retrieval over ocean.

Algorithms, which are capable to derive the cloud optical thickness and separately the aerosol optical thickness for the same partly cloudy pixel currently do not exist.

Our aerosol—cloud algorithm is also not capable to deal with partly cloudy pixels. However, we combined independent aerosol and cloud retrieval algorithms in one processing chain to have a possibility to derive simultaneously aerosol and cloud information in the scene under study (not in a single pixel) using

a single retrieval procedure. The above-mentioned algorithms have been recently developed by the aerosol and cloud research group at the Bremen University for use with data from the Scanning Imaging Absorption Spectrometer for Atmospheric Chartography (SCIAMACHY) aboard the Environmental Satellite (ENVISAT) [7]. ENVISAT was successfully launched on March 1, 2002, and first data have already been delivered to the research community.

The objective of this paper has been to demonstrate some of the capabilities and limitations of the algorithm developed for the studies of the atmospheric optical thickness. For this purpose, the well-proven data from the Sea-viewing Wide Field-of view Sensor (SeaWiFS) on Orbview-2, distributed by NASA Goddard Distributed Active Archive Center, have been used. SeaWiFS measures earthshine radiance in eight channels (0.402–0.422 μm, 0.433–0.453 μm, 0.480–0.5 μm, 0.500–0.520 μm, 0.545–0.565 μm, 0.660–0.680 μm, 0.745–0.785 μm, 0.845–0.885 μm). The swath width is 2801 km (58.3°) for the local area cover (LAC) product and 1502 km (45°) for the global area cover product (GAC). The spatial resolution is 1.1 km for the LAC and 4.5 km for the GAC. Note that the SeaWiFS was successfully applied to ocean color studies [15], [16], [58]. Stamnes *et al.* [53] introduced an algorithm for the simultaneous retrieval of aerosol optical properties and chlorophyll concentrations over oceans using SeaWiFS imagery.

A section of a global area cover data set of Western Europe taken on a cloudy day of October 11, 2001 was selected. It consists of 199×500 pixels with the size approximately 4.5×4.5 km^2 at the nadir observation. Thus, the results obtained are statistically significant. The correspondent file can be downloaded from the NASA Goddard Distributed Active Archive Center (file S2 001 284 113 048L1a_gac at http://daac.gsfc.nasa.gov/data/dataset/SEAWIFS/).

II. AEROSOL OPTICAL THICKNESS AND ANGSTRÖM EXPONENT

A detailed description of the aerosol subsection of the retrieval algorithm is given elsewhere [56], and therefore, only a brief outline of the retrieval procedure is given below.

The aerosol algorithm determines the aerosol reflectance $R_a(\lambda)$ as the function of the wavelength by subtracting the contributions for the Rayleigh path radiance $R_r(\lambda)$ and the contribution from the surface (land or ocean) reflectance $R_s(\lambda)$ from the top-of atmosphere (TOA) reflectance $R_{\text{TOA}}(\lambda)$. Namely, we have: $R_a(\lambda) = R_{\text{TOA}}(\lambda) - R_r(\lambda) - R_s(\lambda)$, where $R_S(\lambda) = (A_{\text{Surf}} t_1 t_2)/(1 - A_{\text{Surf}} r)$. Here, A_{Surf} is the spherical albedo of the surface, r is the spherical albedo of the atmospheric layer, and t_1, t_2 are transmission coefficients for light propagating from the sun to the surface (t_1) and from the surface to satellite (t_2). Functions t_1 and t_2 include both direct and diffused light transmission [33].

Lookup tables for the aerosol reflectance yield the spectral aerosol optical thickness τ_a over oceans ($\lambda \leq 0.86$ μm) and vegetation ($\lambda \leq 0.67$ μm). Constrains are used to minimize the deviation of the aerosol optical thickness from a monotonic spectral behavior. We also find the parameters of the Angström exponential law $\tau_a(\lambda) = \beta \lambda^{-\alpha}$, minimizing the functional $\psi = (\tau_a(\lambda) - \beta \lambda^{-\alpha})^2$.

The algorithm takes into account the digital elevation model to determine the actual surface pressure for the determination of the Rayleigh path reflectance of the observed target [56]. This will be combined in the future with the retrievals using O2 and O4 absorption bands, which are, for example, available from SCIAMACHY [7] data.

The crucial point in any aerosol retrieval scheme is the account for the surface reflection [29], [30], [58]. This is an important issue for aerosol retrievals both over land and ocean. In particular, Kaufman *et al.* [29], [30] proposed to use the correlation between spectral reflectances in visible and near-infrared (e.g., at 2.1 μm) to solve the problem of the aerosol optical thickness determination over land. This approach is routinely used by the MODIS team [8], [32]. This technique, however, cannot be applied to the SeaWiFs instrument due to the lack of the 2.1-μm channel.

Although it is of a general interest to be able to decode the SeaWiFS TOA reflectance in respect to the aerosol optical thickness both over land and ocean.

Our correction for the land surface reflectance is based on the linear mixing of an apparent spectral surface reflectance from a "vegetation" spectrum and a "bare soil" spectrum tuned by the normalized differential vegetation index (NDVI). The different surface spectra used were obtained during the LACE-98 experiment [56].

A measured clear sky backscattered spectrum of the ocean is used to describe the light reflectance from water surfaces [56]. In particular, similarly to the case over land, we present the ocean surface reflectance as a linear mixture of experimentally measured clear water and coastal water spectra tuned by the normalized differential pigment index (NDPI), defined as the the differences of TOA reflection functions at wavelengths 0.443 and 0.555 μm divided by the value of the reflection function at 0.49 μm. The influence of whitecaps is neglected. Due to a comparatively small aerosol loading in the scene under study, the values of r and also the diffused parts of functions t_1 and t_2 are small. Therefore, we keep only direct components of the solar flux in transmissions t_1 and t_2. This simplifies the retrieval. Note that the glint is avoided by the tilt of the instrument.

One can find the flowchart of the procedure in Fig. 1. In particular, note that the cloud free and totally cloud covered pixels are selected and then the optical thickness related to this particular pixel is retrieved. The threshold value of the top-of-atmosphere reflectance function R for the aerosol-cloud pixels discrimination is set to be equal to 0.2 at the spectral range 0.845–0.885 μm (the eighth channel of the SeaWiFS). Values of R less than 0.2 correspond to cloud-free pixels in the algorithm. This is a rather crude estimation as compared to comprehensive state-of-art cloud screening algorithms (e.g., we do not account for the influence of the observation geometry on the threshold value of the top-of-atmosphere reflectance function, etc.). This could lead to the classification of thin cirrus clouds as aerosols and, therefore, to produce wrong retrieval results. However, it should be remembered that the SeaWiFS provides us with only limited spectral information in comparison with more advanced sensors (e.g., MODIS). Therefore, it should be underlined that results for the aerosol optical thickness (especially, for larger values of τ_a) could be biased due to the unidentified presence of clouds in the field of view of the instrument.
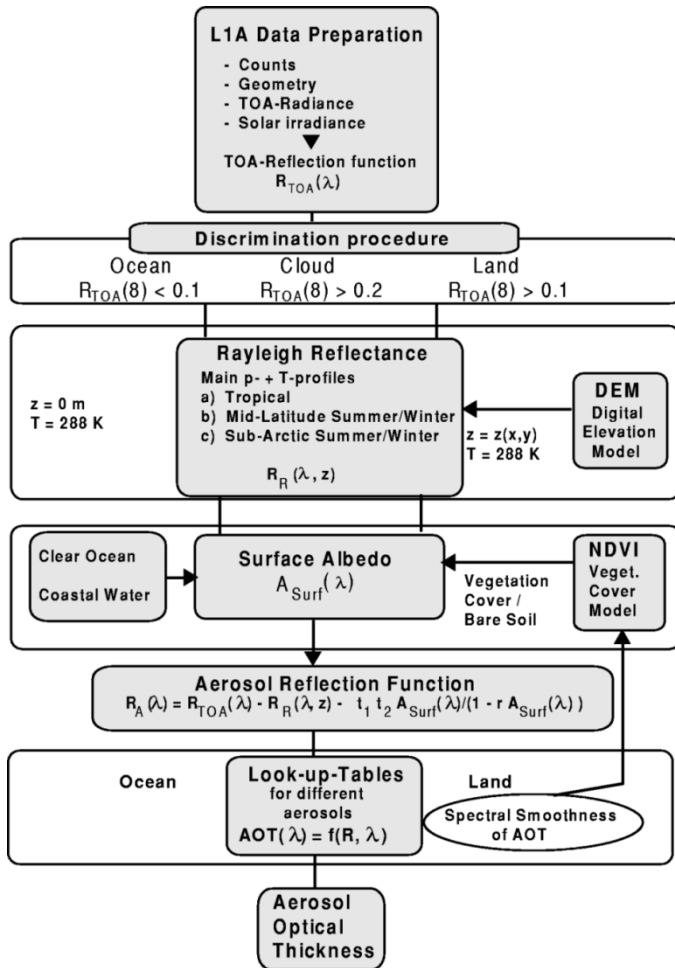
Fig. 1.   Flowchart of the retrieval procedure for the aerosol optical thickness determination.

Fig. 2.   Aerosol optical thickness at the wavelength 0.412 μm. AERONET stations used for the validation are shown by symbols. Black areas correspond to clouds.

A large number of aerosol particles in the terrestrial atmosphere (mainly of mineral origin and sea salt) are irregularly shaped. The use of the Mie theory, which is the basis of the most modern operational aerosol retrieval algorithms, therefore, may result in an inaccurate estimation of the aerosol amount. One important feature of the algorithm developed is the precalculation of lookup tables using the experimentally determined aerosol phase functions for typical atmospheric conditions [56]. These experimentally determined phase functions include the features of light scattering by both spherical and nonspherical (e.g., pronounced side light scattering) aerosol particles. The semiempirical theory of Pollack and Cuzzi [48] was used to derive the aerosol phase function as the best fit for the closure between the measured ground-based spectral optical data (the aerosol optical thickness τ_a and the angular sky brightness distribution in the almucantar). It should be pointed out that the correct account for the aerosol microphysical model (e.g., the shape and size of particles) is an important issue of any aerosol retrieval algorithm (e.g., see Stamnes *et al.* [54]).

The algorithm has as an input the TOA reflectance at channels 1–6 of SeaWiFS (0.412–0.670 μm) for the retrieval of the aerosol optical thickness over land. Channels 6 and 8 are used for the determination of the NDVI and, therefore, the land reflec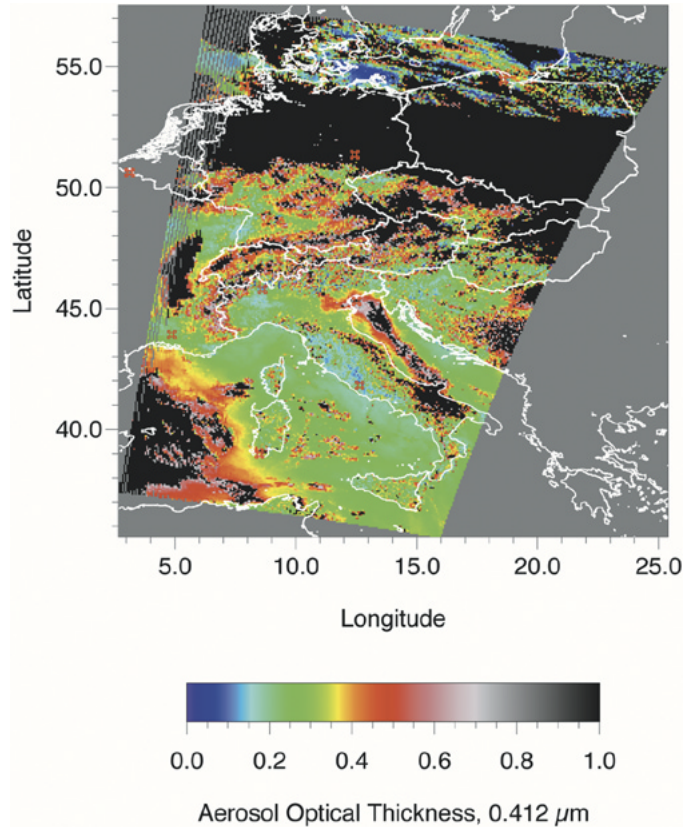tance. Because of the decreasing surface reflectance with decreasing wavelength, the channel 1 (0.412 μm) gives the best results for the aerosol optical thickness retrievals. All eight channels are used for retrievals over water.

The aerosol part of the algorithm was validated by comparing with ground-based measurements. The results of satellite and ground-based techniques differ not more than by 20% and show a sufficient correlation. Details of the validation campaign can be found in [56], where also a full description of the algorithm is presented.

The results of the aerosol optical thickness retrieval are presented in Fig. 2, which show the spatial distribution of τ_a at $\lambda = 0.412$ μm at a given time (11:30 UTC) on October 11, 2001. The clouds are masked as black areas in Fig. 2. The corresponding frequency distributions of the optical thickness is shown in Fig. 3. We also show the frequency distribution of the retrieved value of α (see Fig. 4). The validation of results using AERONET DATA is presented in Fig. 5.

Let us analyze results obtained. The aerosol optical thickness of the scene studied is peaked around the modal value equal to 0.25 (see Fig. 3), which is close to the value of 0.27, reported in [27] for roughly the same region. The ratio s of the half-width of the distribution of τ_a, to the modal value of optical thickness τ_0 is equal approximately to 0.5. The distribution, presented in Fig. 3 may be possibly biased due to the presence of subpixel clouds (see Fig. 2). This fact and also possible additional illumination of a cloudless atmosphere by light, coming from neighboring clouds (see Fig. 2), may result in the over-estimation of the aerosol optical thickness at larger τ.
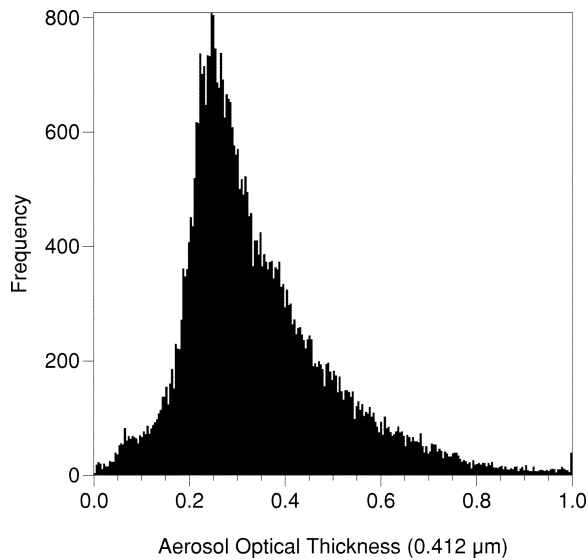
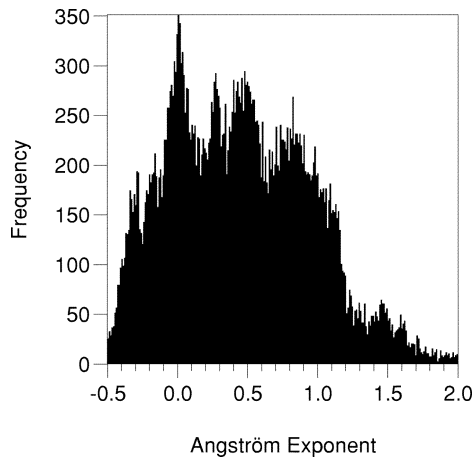Fig. 3. Frequency distribution of the aerosol optical thickness for the scene studied.

Fig. 4. Frequency distribution of the Angström exponent for the scene studied.
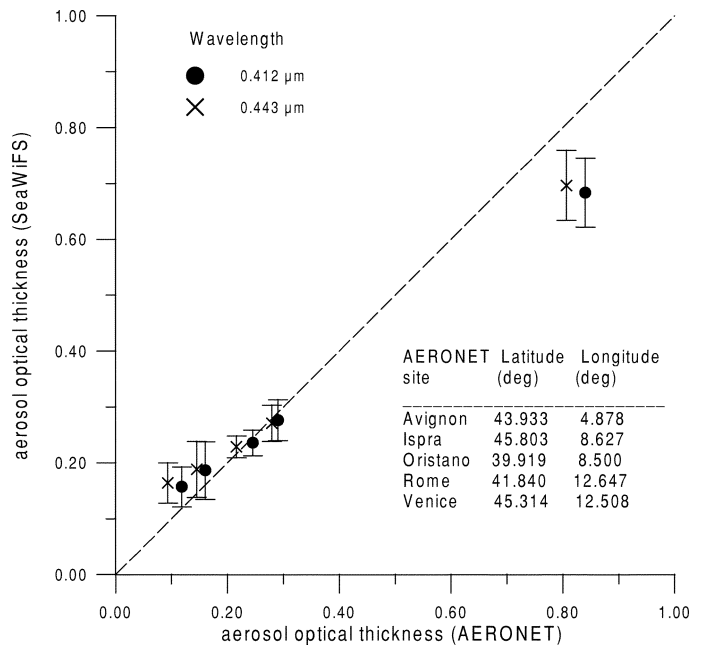

Fig. 5. Retrieved aerosol optical thickness as compared to AERONET data. The AERONET locations can be sorted by the value of the optical thickness. Then we have the following order: Ispra (the smallest value of τ_a), Rome, Avignon, Oristano, Venice.

The regional weather explains the change of τ_a across the scene in Fig. 2. High values of τ_a are present to the south of the cloud front system, whereas the small aerosol optical thickness is observed to the north behind the large cloud field at the rear of the cold front (see Fig. 2).

Fig. 2 indicates that the aerosol optical thickness is smaller behind a cloud system front (over North Sea, Scandinavia, Northern Poland and Baltic Sea). This is best explained by the cleaning effect of atmosphere by clouds. A significant amount of pixels with τ in the range $0.15 \ldots 0.25$ (green and blue color in Fig. 2) is observed over Central Europe, Italy, and the Mediterranean. The aerosol optical thickness over Po Valley in northern Italy reaches values of $0.3 \ldots 0.5$. This large difference (approximately, two times) can be attributed to the anthropogenic activity coupled with the local meteorological situation.

We see that our algorithm is capable to quantify the strength of sources of atmospheric pollution in Western Europe, using τ_a as a convenient indicator of the atmospheric turbidity.

A comparatively large value of the aerosol optical thickness is also observed in the left corner at the bottom of Fig. 2. This is,

possibly, due to the simultaneous existence of a water cloud and a dust outbreak from Sahara. Note that generally dust aerosols and clouds strongly interact, producing a water–mineral aerosol mixture.

In contrast to the optical thickness of cloudy media, the aerosol optical thickness can strongly depend on the wavelength [20]. Thus, the value of τ_a was retrieved not only at the wavelength 0.412 μm, as shown in Fig. 2, but also for several wavelengths in the range 0.412–0.865 μm over water. For pixels over land, only wavelengths 0.412–0.670 μm were used. This is due to a strong light reflection by vegetation for larger wavelengths, which considerably decreases the retrieval accuracy.

The spectral slope of the aerosol optical thickness was retrieved for each cloudless pixel. As one might expect, it was found, that the aerosol optical thickness has different spectral slopes α within the scene. The frequency of occurrence of different Angström exponents α is presented in Fig. 4. Although α is biased both over land and sea due to the insufficient information on the spectral surface reflectance (especially for the channels 0.555 and 0.67 μm), it gives an indication for different aerosol types.

A certain fraction of the atmospheric aerosol has nearly neutral spectral slopes. Similar findings were also reported by Ignatov and Stowe [26] for the case of oceanic aerosols. It means that the size of aerosol particles is comparatively large in the scene studied here. This is, probably, a consequence of the influence of the maritime aerosol or possible cloud formation events in the scene under study. The dust aerosol, which originates due to the atmosphere—land interactions and due to the transport from other regions (e.g., from the Sahara; see bottom of Fig. 2), could be another source of small or even negative values of α.

Other parts of the scene have values of α, which are typical for continental aerosols [20]. The most frequent values of α are found to be in the range $[-0.1, 1.1]$ (see Fig. 4). Note that for continental aerosols the value of α is usually in the range 1.0–1.5 [2], [28], [51]. Deviations from these numbers obtained for our particular case are most probably due to the influence of the maritime aerosol and cloud formation processes, as it was mentioned above. We should underline that values of α in the range $[-0.1; 1.8]$ were reported for maritime aerosol in [38]. Schmidt [51] has obtained values of α in the range $[0.1; 0.4]$ for the clean oceanic aerosol.

Note that operational aerosol retrieval algorithms give values of α in the range [0, 3] and even larger [8]. Our results (and those in [21], [23], [38], [51], and [52]), however, show that values of α larger than 2.0 occur infrequently. This contradiction should be resolved in future research.

Ignatov and Stowe [26] proposed to use the normal distribution for the description of the probability distribution functions of the Angström exponent over oceans. It follows from Fig. 4 that the probability distribution function of the Angström exponent for pixels over land in our case can be also fitted by a normal distribution, if we disregard events with large τ_a. They are most probably due to residual cloud contamination of pixels assumed to be clear.

The frequency distribution of the aerosol optical thickness in Fig. 3 is skewed and have long tails for larger τ_a. This means that they can be approximated by the Gamma or Lognormal distributions even for such large scenes as given in Fig. 2. Such statistical distributions of aerosol and cloud optical thickness have also been reported and used by other research groups [3], [12], [25], [26], [46], [47].

It is of importance to check the accuracy of our retrieval, using ground-based measurements. For this we have used data given by the Aerosol Robotic Network (AERONET) [11], [19]. The AERONET is the number of identical globally distributed sun- and sky-scanning ground-based automated radiometers. They provide measurements of aerosol optical properties, including aerosol optical thickness on a long term basis (up to ten years in some locations). The channels of AERONET instruments (0.34, 0.38, 0.44, 0.5, 0.67, 0.87, and 1.02 μm), however, do not coincide with the channels of the SeaWiFs (0.402–0.422 μm, 0.433–0.453 μm, 0.480–0.5 μm, 0.545–0.565 μm, 0.660–0.680 μm, 0.745–0.785 μm, and 0.845–0.885 μm). So, we made an interpolation between the individual spectral points, where the optical thickness is measured by five AERONET stations located in Avignon, Ispra, Oristano, Rome, and Venice, to have the results for central positions of the SeaWiFs bands. Also, we averaged results of our retrievals for five pixels surrounding the AERONET sites to avoid possible fluctuations in the aerosol spatial distribution. Other AERONET stations placed in Europe gave no data due to the influence of the cloudiness at their sites (see Fig. 2).

Results of comparisons for first two channels of the SeaWiFS instrument are given in Fig. 5. It follows that the results are less accurate for the small optical thickness, which one should expect. There is also the deviation for the comparatively large optical thickness (close to 0.9; see AERONET results). However, we see that the correspondence is generally good for most common values of the aerosol optical thickness (around 0.25) even accounting for the fact that the AERONET measurements are performed at a given point and satellite data refer to much broader area. This underlines a comparatively high accuracy of our aerosol retrieval technique over land for first two channels of the SeaWiFs instrument. We also have compared our satellite retrieval results for larger wavelengths (not shown here). It was found that the difference of the retrieved optical thicknesses as compared to those derived from AERONET generally increases with the wavelength. Most probably, this is related to the fact that only single spectrum of a green vegetation (measured over Germany) is used in our retrieval technique. However, in reality spectra of vegetation could differ considerably. Note that AERONET sites we have selected are located in southern part of Europe, where vegetation (and also terrain) differs from that in Germany. We would like to address discrepancies found in our next publication. The light reflection by vegetation (and also by bare soil) is low for first two channels of SeaWiFs. This makes it possible to make accurate retrievals of the aerosol optical thickness over land for these channels. In particular, we note that the distribution given in Fig. 3 is representative for the aerosol optical thickness over Europe.

III. Cloud Optical Thickness and Spherical Albedo

The cloud optical thickness is found using the asymptotic approach proposed in [31] and [50]. The retrieval is based on the asymptotic solution of the radiative transfer equation at large cloud optical thickness. It has the following form [31]:

$$R(\mu_0, \mu, \phi) = R_\infty(\mu_0, \mu, \phi) - tK(\mu_0)K(\mu) \qquad (1)$$

where the reflection from underlying surface is neglected. Here, μ is the cosine of observation angle, μ_0 is the cosine of the incidence angle, ϕ is the relative azimuth, R_∞ is the reflection function of a semi-infinite layer, $K(\mu)$ is the escape function [55], and t is the global transmittance of a cloud layer, given by the following formula:

$$t = (\sigma + 0.75\tau(1 - g))^{-1}. \qquad (2)$$

Here, g is the asymmetry parameter [31] and σ is the parameter, which is approximately equal to 1.07 for cloud phase functions [31], [34]. The precise definition of functions $R_\infty(\mu_0, \mu, \phi)$ and $K(\mu)$ are given in [55].

The accuracy of (1) is better than 1% for clouds having the optical thickness larger than 10 [31]. Therefore, it provides an excellent approximation for the overcast cloudy conditions (see the black colored area in upper portion of Fig. 2). King [31] validated the algorithm of cloud optical thickness retrieval based on (1) and found a good agreement with airborne experiments (see also [43]).

We assume here that clouds are composed of water droplets, characterized by the Deirmendjian's Cloud C1 droplet size distribution [9]. As the modified asymptotic theory is accurate only at $\tau \geq 10$, large retrieval errors can result for smaller cloud optical thickness. However, thin clouds often consist of ice crystals. Also, as optically thin clouds are highly inhomogeneous, the application of the standard radiative transfer equation for a

homogeneous plane-parallel layer is not justified and may lead to large retrieval errors [36], [37]. Generally, radiative properties of inhomogeneous clouds are poorly understood. So, this study is mostly limited to the case of optically thick clouds. A band of a such cloud field is seen in the upper part of Fig. 1.

The retrieval of the cloud optical thickness is performed at the wavelength $0.412\,\mu$m, where the reflection of light from the vegetation, bare soil, and water can be neglected. However, due to the large size of cloud droplets as compared to the wavelength, the optical thickness in visible almost does not depend on the wavelength. So, results obtained can be safely extrapolated at least for the whole visible part of the electromagnetic spectrum.

The equation for the cloud optical thickness follows from (1) and (2) after simple algebraic calculations. In particular, we have from (2)

$$\tau = \frac{4}{3}\frac{t^{-1} - \sigma}{1 - g} \qquad (3)$$

where [see (1)]

$$t = \frac{R_\infty(\mu_0, \mu, \phi) - R(\mu_0, \mu, \phi)}{K(\mu_0)K(\mu)}. \qquad (4)$$

Note that the accuracy of the retrieval according to (3) decreases as t decreases. The spatial distribution of the cloud optical thickness derived using (3) is shown in Fig. 6.

It was assumed that $g = 0.85$, which is the case for most of water clouds. $R_\infty(\mu_0, \mu, \phi)$ was calculated using the code described in [40] for the Cloud C1 gamma distribution of water droplets [9], having the effective size $6\,\mu$m and $\lambda = 0.412\,\mu$m. This assumption does not influence the result of the retrieval, however. This is because of low sensitivity of the function $R_\infty(\mu_0, \mu, \phi)$ to the size of droplets [34]. Also, we used the approximation

$$K(\mu) = \frac{3}{7}(1 + 2\mu) \qquad (5)$$

which is valid with the relative error less than 2% at μ greater than 0.2 [34] for arbitrary phase functions.

Note in passing that (3) can also be used for the determination of the cloud optical thickness from airborne measurements of the reflected solar flux [33]: $r(\mu_0) = 2\int_0^1 R(\mu, \mu_0)\mu d\mu$, where $R(\mu, \mu_0)$ is the azimuthaly averaged reflection function. Then, we have [33]: $r(\mu_0) = 1 - tK(\mu_0)$ for a nonabsorbing wavelength and therefore

$$t = \frac{1 - r(\mu_0)}{K(\mu_0)}. \qquad (6)$$

So, rather complex calculations of $R_\infty(\mu_0, \mu, \phi)$ are avoided in this case. This is an important point.

Turning to the analysis of cloud optical thickness distribution derived, we note that the cloudiness in the terrestrial atmosphere is best described as a persistent and extensive background of optically thin clouds mixed together with highly variable component of optically thick (and often precipitating) clouds, which are very sparse [49]. Namely this case corresponds to the scene studied (see Fig. 2), where the band of the optically thick cloud field propagates from the North-West to the East in agreement
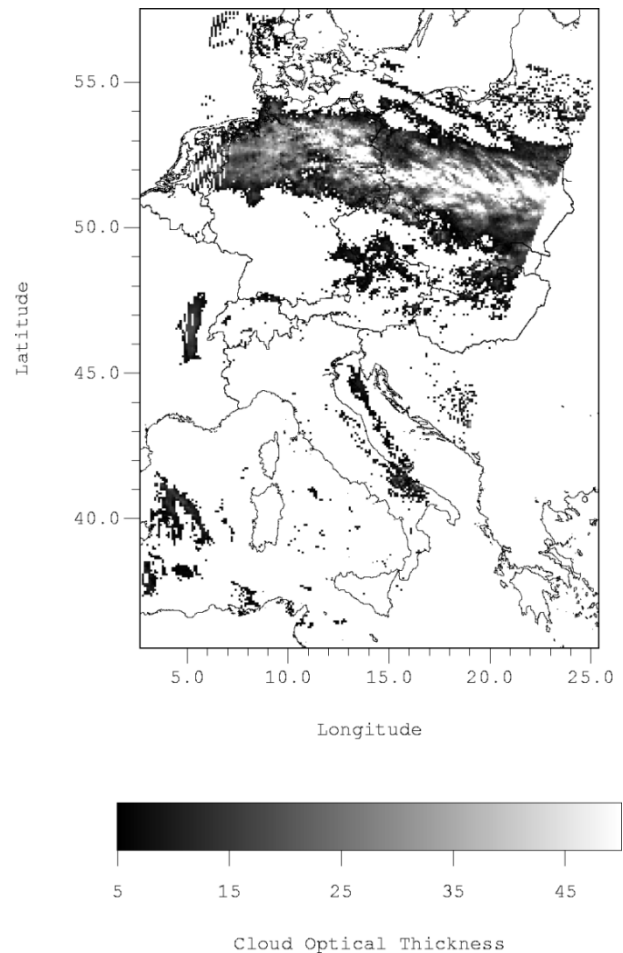

Fig. 6. Cloud optical thickness spatial distribution for the scene studied. The fractal structure in the middle of the cloud band is clearly seen.

with other satellite observations (e.g., see the weather map for this day at http://www.wetter.zentrale.de/topkarten).

Note that winds are mostly eastward in midlatitude regions. Thus, the maritime aerosol with almost neutral spectral slopes are often observed in many areas of the Western Europe. It also confirmed by this study. This is also the reason for comparatively large aerosol concentrations, e.g., over Eastern Europe as compared to the Western Europe [6]. Larger aerosol concentrations influence the cloud droplet spectra, precipitation, and concentrations of droplets and crystals in clouds [6], [44].

The study of the cloud field shows that the modal cloud optical thickness in the brightest part of the cloud band in Fig. 6 is around 30 (see Fig. 7).

Note that (4) can be used for the calculation not only the global cloud transmittance but also the cloud spherical albedo $r = 1 - t$, which is an important parameter for climate studies. It gives a hemispherical reflectance of a cloud layer. Then the additional information on the value of g is not required to run the retrieval procedure. This is an important point.

We have derived the spatial spherical albedo distribution over the cloudy portions of the image studied. This distribution (not shown here) is similar to that of the cloud optical thickness given in Fig. 6. The frequency distribution of the cloud spherical albedo in the scene (see Fig. 8) differs considerably from the correspondent frequency distribution for the cloud optical
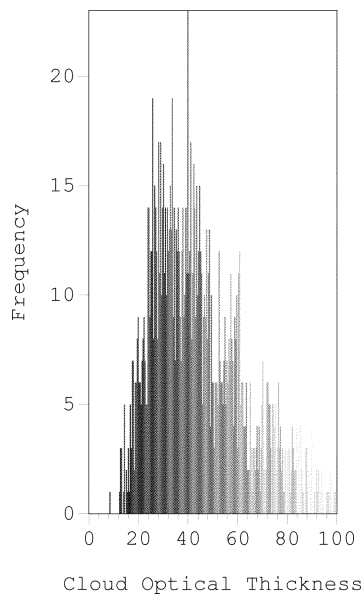
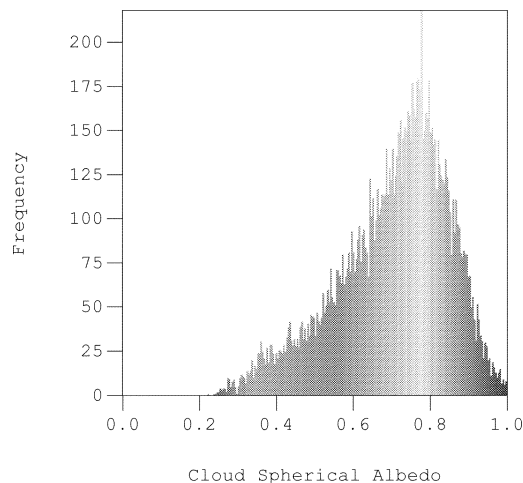Fig. 7. Cloud optical thickness frequency distribution.

Fig. 8. Cloud spherical albedo frequency distribution for the scene studied.

thickness shown in Fig. 7. The maximum of the spherical albedo distribution is located around 0.8 for the case under study.

The distribution itself can be described by the well-known beta distribution, which corresponds to similar findings in [35]. However, their results are based on pixel brightness studies for a given solar angle and observation geometry. Our results, presented in Fig. 8 correspond to the angle-independent spherical albedo. Note that the betta distribution usually appears if there is a boundary for the physical value studied. In our case, for example, cases with $r > 1$ are not possible due to physical reasons.

IV. CONCLUSION

The atmospheric optical thickness over land and water surfaces has been retrieved, using newly developed aerosol-cloud retrieval algorithm.

Note that our algorithm is not capable to deal with partly cloudy pixels. The cloudy part of the joint algorithm works only for clouds having optical thickness larger than approximately 5. The aerosol part of the technique can be applied for studies of

aerosol optical thickness distributions both over land and ocean. However, land surfaces with large reflectance (e.g., snow fields and deserts) should be avoided. Then the aerosol signal is too small as compared to the surface contribution. This does not allow to get meaningful results using SeaWiFS imagery.

The most probable cloud optical thickness observed for the extended cloud field in Fig. 2 is around 30 (see Fig. 7). Note also that one can observe a fractal structure in the middle of the cloud band in Fig. 6. The most probable value of the aerosol optical thickness is equal to 0.25 (see Fig. 3). Note also the large variability of τ_a and regional differences in the scene (see Fig. 2).

The results reported in this paper have a high accuracy for large $(\tau > 10)$ optical thickness. Generally speaking, lookup tables should be used in the case of thin clouds. However, the question arises if the exact radiative transfer theory for plane-parallel layers can be applied in the case of thin clouds at all. This obstacle is due to the pronounced stochastic nature of thin clouds. The problem should be checked and clarified in future research (see [3]–[5], [36], [37], and [39]). We have also retrieved the cloud optical thickness outside the extended cloud field in the upper portion of Fig. 6. However, results obtained are most probably biased due to errors in (1) for the smaller values of the optical thickness.

The data presented here (e.g., see Figs. 2 and 6) can be used for the comparison of different aerosol/cloud retrieval algorithms, existing worldwide. Such studies are needed to overcome the current complexity, associated with the theory and practice of the cloud and aerosol remote sensing in the terrestrial atmosphere.

Note that application of our algorithm reveals some important issues to address in future. First of all we note that the aerosol optical thickness tends to be uniform outside industrial areas and special events like fires, outbreaks from deserts and volcanic activity. Therefore, highly variable aerosol optical thickness distribution shown in Fig. 2 is, probably, due to the cloud formation influence. It means that further study of the cloud threshold in the aerosol retrieval scheme is needed. Further, the spatial distribution of the Angström exponent (not shown here) differs significantly from the average data for continental areas ($\alpha = 1.3$ [28]). This is, probably, due to the influence of maritime aerosol and cloud formation processes taking place in a given scene as well. On the other hand, it could be also partially due to the surface variability, which is taking into account only approximately in our algorithm. Our surface reflection model should be further improved, therefore.

Due to the limited spectral range of the SeaWiFS instrument it is not possible to retrieve other cloud parameters such as cloud top height, cloud liquid water path, cloud droplet effective radius, cloud geometrical thickness, cloud thermodynamic phase (and similar parameters for the atmospheric aerosol). We also have worked out the extension of our algorithm to treat these more complex retrievals, using spectral distribution of backscattered light for cloudy scenes in visible and near-infrared spectral ranges (e.g., see [34]).

Our next task is to apply our retrieval scheme to aerosol—cloud media in different geographical locations for different seasons. This will enable us to gain an important statistical information on cloud—aerosol interactions and properties.

In conclusion, we note, that extensive satellite retrievals of atmospheric turbidity given by τ (and also other aerosol and cloud micro- and macrophysical parameters, e.g., particle size distributions and shapes, cloud-top-heights and cloud geometrical thicknesses, cloud thermodynamical state, etc.) provide the statistical data on the required temporal and regional variability of suspended matter in the atmosphere of our planet. This information along with the data on the concentrations and variability of trace gases [7] is of a paramount importance for modern atmospheric chemistry and physics as well as climate change studies [24].

ACKNOWLEDGMENT

REFERENCES

[1] B. A. Albrecht, "Aerosols, cloud microphysics and fractional cloudiness," *Science*, vol. 245, pp. 1227–1230, 1989.

[2] A. Angstrom, "On the atmospheric transmission of sun radiation: II," *Gografiska Annaler*, vol. 12, pp. 130–159, 1930.

[3] H. W. Barker *et al.*, "A parameterization for computing grid-averaged solar fluxes for inhomogeneous marine boundary layer clouds, II, Validation using satellite data," *J. Atmos. Sci.*, vol. 53, pp. 2304–2316, 1996.

[4] ——, "Optical depth of overcast cloud across Canada: Estimates based on surface pyranometer and satellite measurements," *J. Climate*, vol. 11, pp. 2980–2994, 1998.

[5] ——, "Inference of cloud optical depth from aircraft-based solar radiometric measurements," *J. Atmos. Sci.*, vol. 59, pp. 2093–2111, 2002.

[6] F.-M. Breon *et al.*, "Aerosol effect on cloud droplet size monitored from satellite," *Science*, vol. 295, pp. 834–841, 2002.

[7] H. Bovensmann *et al.*, "SCIAMACHY: Mission objectives and measurement modes," *J. Atmos. Sci.*, vol. 56, pp. 127–150, 1999.

[8] D. A. Chu *et al.*, "Validation of MODIS aerosol optical depth retrieval over land," *Geophys. Res. Lett.*, vol. 26, no. 12, Dec. 2002.

[9] D. Deirmendjian, *Electromagnetic Scattering on Spherical Polydispersions*, Amsterdam, The Netherlands: Elsevier, 1969.

[10] J. L. Deuze, M. Herman, P. Goloub, D. Tanre, and A. Marchand, "Characterization of aerosol over ocean from POLDER/ADEOS-1," *Geophys. Res. Lett.*, vol. 26, pp. 1421–1424, 1999.

[11] O. V. Dubovik *et al.*, "Variability of absorption and optical properties of key aerosol types observed in worldwide locations," *J. Atmos. Sci.*, vol. 59, no. 1, pp. 590–608, 2002.

[12] Q. Fu, B. Carlin, and G. Mace, "Cirrus horizontal inhomogeneity and OLR bias," *Geophys. Res. Lett.*, vol. 27, pp. 3341–3344, 2000.

[13] P. Goloub, D. Tanre, J. L. Deuze, M. Herman, A. Marchand, and F. M. Breon, "Validation of the first algorthm applied for the aerosol properties over the oceans using POLDER/ADEAOS measurements," *IEEE Trans. Geosci. Remote Sensing*, vol. 37, pp. 1586–1595, May 1999.

[14] H. R. Gordon and M. Wang, "Retrieval of water-living radiance and aerosol optical thickness over the oceans with SeaWiFS: A preliminary algorithm," *Appl. Opt.*, vol. 33, pp. 443–452, 1994.

[15] H. R. Gordon, "Atmospheric correction of ocean color imagery in the Earth observation system era," *J. Geophys. Res.*, vol. 102, pp. 17 081–17 106, 1997.

[16] ——, "Pitfalls in atmospheric correction of ocean color imagery: How should aerosol optical properties be computed?: Comment," *Appl. Opt.*, vol. 42, pp. 542–544.

[17] Q. Han *et al.*, "Three different behaviors of liquid water path of water clouds in aerosol-cloud interactions," *J. Atmos. Sci.*, vol. 59, pp. 726–735, 2002.

[18] Q. Harshvardan *et al.*, "Aerosol influence on cloud microphysics examined by satellite measurements and chemical transport modeling," *J. Atmos. Sci.*, vol. 59, pp. 714–725, 2002.

[19] B. N. Holben *et al.*, "AERONET—A federated instrument network and data archive for aerosol characterization," *Remote Sens. Environ.*, vol. 66, pp. 1–16, 1998.

[20] ——, "An emerging ground-based aerosol climatology: Aerosol optical depth from AERONET," *J. Geoph. Res.*, vol. D106, pp. 12.067–12.097, 2001.

[21] W. A. Hoppel *et al.*, "Aerosol size distributions and optical properties found in the marine boundary layer over the Atlantic Ocean," *J. Geophys. Res.*, vol. D95, pp. 3659–3686, 1990.

[22] R. B. Husar, J. M. Prospero, and L. L. Stowe, "Charaterization of troposperic aerosols over the oceans with the NOAA AVHRR optical thickness product," *J. Geophys. Res.*, vol. 102, pp. 16 889–16 909, 1997.

[23] T. Elias, "Polarising properties of the aerosols on the north-eastern tropical Atlantic Ocean, with emphasis on the ACE-2 period," *Tellus*, vol. 52B, pp. 620–635, 2000.

[24] IPCC, "Climate change, 2001: The scientific basis," Cambridge Univ. Press, Cambridge, U.K., 3rd Rep. IPCC, 2001.

[25] A. Ignatov and L. Stowe, "Aerosol retrievals from individual AVHRR channels. Part I: Retrieval algorithm and transition from Dave to 6S radiative transfer model," *J. Atmos. Sci.*, vol. 59, pp. 313–336, 2002a.

[26] ——, "Aerosol retrievals from individual AVHRR channels. Part II: Quality control, probability distribution functions, information content, and consistency checks of retrievals," *J. Atmos. Sci.*, vol. 59, pp. 335–362, 2002b.

[27] A. Jeuken *et al.*, "Simulation of the aerosol optical depth over Europe for August 1997 and a comparison with observations," *J. Geophys. Res.*, vol. 106, pp. 28 295–28 311, 2001.

[28] C. E. Junge, *Air Chemistry and Radioactivity*. New York: Academic, 1963.

[29] Y. Kaufman *et al.*, "Operational remote sensing of tropospheric aerosol over the land from EOS-MODIS," *J. Geophys. Res.*, vol. D102, pp. 17 051–17 061, 1997a.

[30] ——, "The MODIS 2.1 μm channel—Correlation with visible reflectance for use in remote sensing of aerosol," *IEEE Trans. Geosci. Remote Sensing*, vol. 35, pp. 1286–1298, Sept. 1997.

[31] M. D. King, "Determination of the scaled optical thickness of clouds from reflected solar radiation measurements," *J. Atmos. Sci.*, vol. 44, pp. 1734–1751, 1987.

[32] M. D. King *et al.*, "Remote sensing of cloud, aerosol, and water vapor properties from the Moderate Resolution Imaging Spectrometer (MODIS)," *IEEE Trans. Geosci. Remote Sensing*, vol. 30, pp. 2–27, Jan. 1992.

[33] A. A. Kokhanovsky, *Light Scattering Media Optics: Problems and Solutions*. Chichester, U.K.: Springer-Praxis, 2001.

[34] A. A. Kokhanovsky *et al.*, "A semi-analytical cloud retrieval algorithm using backscattered radiation in 0.4–2.4 spectral region," *J. Geophys. Res.*, vol. D1, no. 4008, 2003.

[35] I. Koren and J. H. Joseph, "The histogram of the brightness distribution of clouds in high-resolution remotely sensed images," *J. Geophys. Res.*, vol. 105, pp. 29 369–29 377, 2000.

[36] N. G. Loeb and R. Davies, "Observational evidence of plane parallel biases: Apparent dependence of cloud optical depth on solar zenith angle," *J. Geophys. Res.*, vol. 1001, pp. 1621–1634, 1996.

[37] N. G. Loeb and J. A. Coakley, Jr., "Inference of marine stratus cloud optical depths from satellite measurements: Does 1D theory apply?," *J. Atmos. Sci.*, vol. 11, pp. 215–233, 1998.

[38] K. Masuda *et al.*, "Use of polarimetric measurements of the sky over the ocean for spectral optical thickness retrieval," *J. Atmos. Oceanic Technol.*, vol. 16, pp. 846–859, 1999.

[39] Q. Min and L. C. Harrison, "Cloud properties derived from surface MFRSR measurements and comparison with GOES results at the ARM SGP site," *Geophys. Res. Lett.*, vol. 23, pp. 1641–1644, 1996.

[40] M. I. Mishchenko *et al.*, "Bidirectional reflectance of flat, opticalyy thick particulate layers: An efficient radiative transfer solution and applications to snow and soil surfaces," *J. Quant. Spectrosc. Radiat. Transf.*, vol. 63, pp. 409–432, 1999.

[41] C. Moulin, F. Guillard, F. Dulac, and C. E. Lambert, "Long-term daily monitoring of Saharan dust load over ocean using METEOSAT ISCCP-B2 data," *J. Geophys. Res.*, vol. 102, pp. 16 947–16 958, 1997.

[42] T. Nakajima and A. Higurashi, "AVHRR remote sensing of aerosol optical properties in the Persian Gulf region, summer 1991," *J. Geophys. Res.*, vol. 102, pp. 16 935–16 946, 1997.

[43] T. Nakajima *et al.*, "Determination of the optical thickness and effective particle radius of clouds from reflected solar radiation measurements. Part II: Marine stratocumulus observations," *J. Atmos. Sci.*, vol. 48, pp. 728–749, 1991.

[44] ——, "A possible correlation between satellite-derived cloud and aerosol microphysical parameters," *Geophys. Res. Lett.*, vol. 28, pp. 1171–1174, 2001.

[45] C. D. O'Dowd *et al.*, "The effect of clouds on aerosol growth in the rural atmosphere," *Atmos. Res.*, vol. 54, pp. 201–221, 2000.

[46] N. T. O'Neill *et al.*, "The lognormal distribution as a reference for reporting aerosol optical depth statistics; empirical tests using multi-year, multi-site AERONET sun photometer data," *Geophys. Res. Lett.*, vol. 27, pp. 3333–3336, 2000.

[47] R. Pincus and S. Klein, "Unresolved spatial variability and microphysical process rates in large-scale models," *J. Geophys. Res.*, vol. 105, no. 27, pp. 27 059–27 065, 2000.

[48] J. B. Pollack and J. N. Cuzzi, "Scattering by nonspherical particles of size comparable to the wavelength: A semi-empirical theory and its application to tropospheric aerosol," *J. Atmos. Sci.*, vol. 37, pp. 868–881, 1980.

[49] W. B. Rossow and R. A. Schiffer, "Advances in understanding clouds from ISCCP," *Bull. Amer. Meteorol. Soc.*, vol. 80, pp. 2261–2287, 1999.

[50] G. V. Rozenberg *et al.*, "The determination of optical characteristics of clouds from measurements of the reflected solar light using data from the Sputnik "KOSMOS-320"," *Izv. USSR Acad Sci., Atmos. Oceanic Phys.*, vol. 10, pp. 14–24, 1978.

[51] T. Schmidt, "Validierung von Aerosolmodellen aufgrund von experimentellen Ergebnissen," Ph.D. thesis, Bremen Univ., Bermen, Germany, 1999.

[52] A. Smirnov *et al.*, "Aerosol optical depth over the oceans: Analysis in terms of synoptic air mass types," *J. Geophys. Res.*, vol. 100, pp. 16 639–16 650, 1995.

[53] K. Stamnes *et al.*, "Pitfalls in atmospheric correction of ocean color imagery: How should aerosol optical properties be computed?: Reply comment," *Appl. Opt.*, vol. 42, pp. 542–544, 2003.

[54] ——, "Accurate and self-consistent ocean color algorithm: Simultaneous retrieval of aerosol optical properties and chlorophyll concentrations," *Appl. Opt.*, vol. 42, pp. 939–951, 2003.

[55] H. C. van de Hulst, *Multiple Light Scattering*. New York: Academic, 1980.

[56] W. Von Hoyningen-Huene *et al.*, "Retrieval of aerosol optical thickness over land surfaces from top-of-atmosphere radiance," *J. Geophys. Res.*, vol. D9, no. 108, p. 4260, 2003.

[57] B. Wielicki *et al.*, "Evidence for large decadal variability in the tropical mean radiative energy budget," *Science*, vol. 295, pp. 841–844, 2002.

[58] B. Yan *et al.*, "Evaluation of a reflectance model used in the SeaWiFS ocean color algorithm: Implications for chlorophyll concentration retrievals," *Appl. Opt.*, pp. 6243–6259, 2002.

Wolfgang von Hoyningen-Huene received the Ph.D. degree from Leipzig University, Leipzig, Germany, in 1976. His Ph.D. work was devoted to the multidimensional statistical analysis of geophysical data. His Habilitation thesis (Leipzig University, 1985) was related to the development of techniques for the determination of optical properties of atmospheric aerosol using ground-based radiometric measurements.

He is currently a member of MERIS/ENVISAT algorithm development team. His main subjects include aerosol optics, satellite retrieval techniques, and inverse problems solutions. He also performs ground-based radiometric measurements.
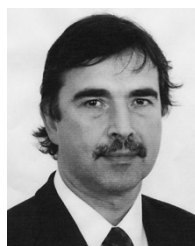
Dr. von Hoyningen-Huene is a member of the German Meteorological Society and the European Aerosol Society.

Heinrich Bovensmann received the Ph.D. degree in nonlinear laser spectroscopy of the dynamics of small molecules from the University of Hannover, Hannover, Germany, in 1994.

Since 1995, he has been a Research Scientist at the Institute of Environmental Physics and Remote Sensing (IUP/IFE), University of Bremen, Bremen, Germany, in the field of stratospheric photochemistry modeling and remote sensing of atmospheric parameters from space-based UV-VIS-NIR measurements. He is member of the SCIAMACHY Science Advisory Group and has advised the SCIAMACHY project in the fields of instrument development, mission planning, and scientific applications. He is Leading Co-Proposer of GeoSCIA, an innovative concept to measure trace gas distributions from geostationary orbit with subhourly temporal resolution. He is currently Head of the SCIAMACHY team at University of Bremen and is involved in several national and international projects.

Dr. Bovensmann is a member of the American Geophysical Union.

Alexander A. Kokhanovsky received the B.A. and M.S. degrees in theoretical physics from the Belarussian State University, Minsk, Belarus, in 1983, and Ph.D. degree in optical sciences from the B.I. Stepanov Institute of Physics, National Academy of Sciences of Belarus, Minsk, Belarus, in 1991. His Ph.D. work was devoted to modeling light scattering properties of various aerosol media and foams.

He is currently a member of the SCIAMACHY/ENVISAT algorithm development team at the Institute of Environmental Physics, University of Bremen, Bremen, Germany. His research interests are directed toward modeling light propagation and scattering in terrestrial atmosphere. He is the author of the books *Light Scattering Media Optics: Problems and Solutions* (Chichester, U.K.: Springer-Praxis, 1999, 2001) and *Polarization Optics of Random Media* (Berlin, Germany: Springer-Praxis, 2003). He has published more than 70 papers in the field of environmental optics, radiative transfer, and light scattering.

Dr. Kokhanovsky is a member of the American Geophysical Union and the Belarussian Physical Society.

John P. Burrows received the B.A. degree in natural sciences and the Ph.D. degree in chemistry, both from Trinity College, Cambridge University, Cambridge, U.K., in 1975 and 1978, respectively, the latter for his studies on free radical reactions by means of laser magnetic resonance spectroscopy.

He has worked at the Harvard Center for Astrophysics, the Environmental and Medical Sciences Division of the UKAEA, the Physical Chemistry Laboratory of Oxford University, and the Max Planck Institute for Chemistry. He has been Professor of atmospheric physics and remote sensing at the Institute of Remote Sensing, Bremen University, Bremen, Germany, since 1992 and is a Visiting Scientist at NASA Goddard Space Flight Center, Greenbelt, MD, SFC since 1994. He is the Principal Investigator/Lead Scientist of the GOME and SCIAMACHY projects and the GeoSCIA/GeoTROPE initiatives.

Dr. Burrows is a member of the American Geophysical Union, the American Chemical Society, and the German Physical Society.